Lasers in Eng., Vol. 29, pp. 197–213
Reprints available directly from the publisher
Photocopying permitted by license only

Characterization of Laser Deposited Ti6Al4V/TiC Composite Powders on a Ti6Al4V Substrate

R.M. MAHAMOOD[1,2,*], E.T. AKINLABI[1], M. SHUKLA[3,4] AND S. PITYANA[5]

[1]*Department of Mechanical Engineering Science, University of Johannesburg, Auckland Park Kingsway Campus, Johannesburg, 2006, South Africa*
[2]*Department of Mechanical Engineering, University of Ilorin, Nigeria*
[3]*Department of Mechanical Engineering Technology, University of Johannesburg, Doornfontein Campus, Johannesburg, 2006, South Africa*
[4]*Department of Mechanical Engineering, MNNIT Allahabad UP, 211004, India*
[5]*National Laser Centre of Council for Scientific and Industrial Research (CSIR), Pretoria, 0001, South Africa*

This paper reports the material characterization of Ti6Al4V/TiC composite produced by laser metal deposition. The Ti6Al4V/TiC composites were deposited with a composition ratio of 50 wt.% Ti64l4V and 50 wt.% TiC. The depositions were achieved by delivering the two powders from a powder feeder consisting of two different hoppers and each hopper contains each of the powders. A total of eight experiments were performed, the scanning speed was kept constant at 0.005 m/s and the laser power varied between 0.4 and 3.2 kW. The gas flow rate and the powder flow rates were also kept at constant settings of 1.44 g/min and 1 l/min respectively for each hopper. The deposits were laterally sectioned, metallographically prepared and characterized through microstructural evaluation, microhardness and wear resistance performance. The effects of varying the laser power on the resulting properties of the composites were studied extensively. The microstructure consists of un-melted carbide (UMC) in the matrix of alpha and prior beta grain structure of Ti6Al4V, and in varying degrees in all the samples. The results showed that the microhardness and the wear resistance performance were dependent on the laser power.

Keywords: coefficient of friction, laser material deposition (LMD), laser metal deposition, material characterization, Nd:YAG laser, Ti6Al4V, Ti64/TiC composite, wear resistance

*Corresponding author: Phone: +27 (0)11 559 4555; E-mail: mahamoodmr2009@gmail.com, mahamoodmr@unilorin.edu.ng

1 INTRODUCTION

Laser material deposition (LMD) belongs to a class of directed energy deposition process according to F42 committee on additive manufacturing (AM) standards [1]. LMD processes builds up components by adding materials layer by layer, according to the path defined by the geometry of the computer aided design (CAD) model data of the component being built [2]. LMD, like any other additive manufacturing technique, has the advantage of building a very complex part at no extra expense and in one single step. This is not possible with the traditional manufacturing processes, which need to break down a complex component into various parts that are later assembled. Also, the traditional manufacturing processes are energy intensive [3] and they generate lots of scrap when producing complex parts. LMD has the advantage of producing a complex component with minimum materials, energy and at low overall cost. Out of all the family of AM technologies, directed energy deposition (DED), of which LMD belongs, is the only class that can be used to repair worn out components. LMD can also be used to build new part on an existing old part with good metallurgical bonding, as against the mechanical bonding achieved with traditional manufacturing methods [1]. LMD can also be used to fabricate parts with dissimilar materials making it suitable for producing composite materials. The use of energy from the laser for material deposition process is very popular in the research community. This is because of the highly collimated nature of laser and the ease of controlling the laser beam to only the required area. Aerospace industry will benefit more from the LMD technology because it is capable of reducing the buy-to-fly-ratio [4], thereby reducing the cost of production, the weight of the aircraft through elimination of parts assembly as well as reducing the running cost of the aircraft.

Ti6Al4V is a Ti alloy grade five, and it is the most widely used Ti alloy in the aerospace industry because of its high specific strength to weight ratio and good corrosion resistance [5]. Despite all these good properties, Ti and its alloys have poor wear resistance properties because they are reactive to contacting surfaces. Ti and its alloys are generally referred to as difficult to machine materials. The use of the LMD to process these materials has provided a better alternative manufacturing technique. Also, the flexibility offered by the LMD makes it possible to produce composite materials [6].

A lot of work on laser deposition and modification of Ti/Ti carbide composite has appeared in the literature [7-11]. Dalili *et al* [7] in a research study on improving the wear resistance of Ti6Al4V/TiC composites through thermal oxidation found that the thermal oxidation treatment resulted in a significant reduction of the wear rates of the composites especially at higher loading conditions. They concluded that the thermal oxidation employed improved the wear properties of the composites. Wang *et al* [8, 9] also established the suitability of using the LMD process to produce composite and

functionally graded material of Ti6Al4V and TiC. They reported that the preliminary sliding wear tests conducted on the Ti6Al4V samples, revealed that the tribological properties of the samples were improved by the reinforced TiC particles.

The underlying physics of the LMD process is yet to be fully understood and there is less work on studying the effect of the processing parameters on the resulting properties of the Ti6Al4V/TiC composite. This study therefore, investigates the effect of laser power on the wear resistance property of the laser deposited Ti6Al4V/TiC composite at low scanning speeds. The microstructure, microhardness, phases, and the wear properties were extensively studied and the results are presented and discussed.

2 EXPERIMENTAL METHODS

2.1 Material details

Hot rolled Ti6Al4V, $72 \times 72 \times 5$ mm^3 thick plates of 99.6% purity, was used as the substrate. The particle size of the Ti6Al4V powder ranged between 150 to 200 μm and also of 99.6% purity. The TiC powder is of an average particle size of 60 μm. Ar gas was used as the carrier gas for the two powders. A glove box was improvised to prevent the deposit from atmospheric contamination of O_2 and N_2. The glove box was filled with the Ar gas, to keep the O_2 level below 10 ppm. The substrate was sandblasted and cleaned with acetone prior to deposition. The schematic of the laser deposition process is shown in Figure 1.

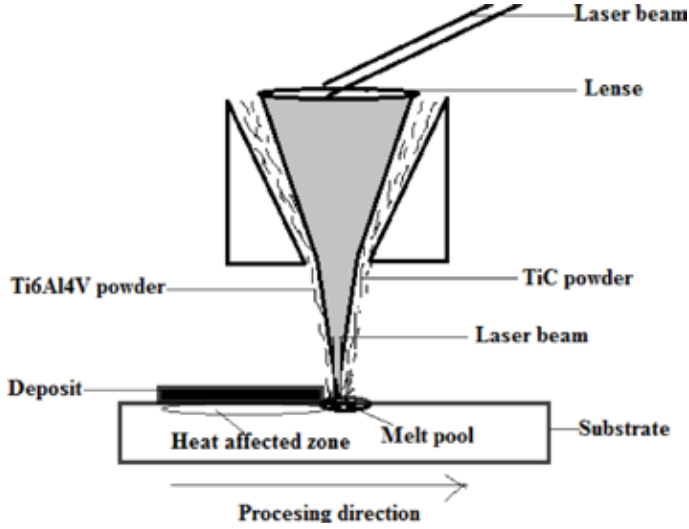

FIGURE 1
Schematic diagram of the LMD process.

2.2 Laser processing details

The Ti6Al4V and TiC powders were delivered into the laser melt pool by a powder feeder. The powder feeder has two hoppers and each hopper was carrying each of the powders. The two powders were delivered into the melt pool simultaneously. The deposition process was achieved by a robot (KR 6-2; KUKA Robotics Corporation) carrying a 4.4 kW Nd:YAG laser (Powerline L-400; Rofin Sinar, GmbH). The end effector of the robot also has the coaxial powder nozzles attached to it. The substrate was fixed in place, while the robot moved to perform the deposition process. The spot size was maintained at 2 mm, which was at a focal distance of 195 mm above the substrate. The powders placed separately in each hopper, has the powder flow rate maintained at 1.44 g/min giving rise to a composite of 50 wt.% TiC and 50 wt.% Ti6Al4V. The gas flow rate was also maintained at 1 l/min for each of the powders. The scanning speed was maintained at 0.005 m/s. The laser power was varied between 0.4 to 3.2 kW (see Table 1 for the processing parameters). Multiple tracks were deposited with 50% overlap for each of the settings in Table 1.

2.3 Analysis and characterization procedures

After the deposition process the samples were cut laterally to reveal the cross-sections. The cut samples were mounted, ground, polished and etched according to the standard metallographic preparation of Ti and its alloys. The samples were observed under the Olympus optical microscope (BX51M; Olympus, Ltd.) and scanning electron microscope (SEM) (VEGA, TESCAN, A.S.) equipped with the energy dispersion spectrometry (EDS) (AZtecEnergy; Oxford Instruments, Ltd.). The X-ray diffraction analysis was performed using X-ray diffractometer (XRD) (Ultima IV; Rigaku Corporation) to study the phases present.

TABLE 1
Processing parameters.

Sample Designation	Laser Power (kW)
A	0.4
B	0.8
C	1.2
D	1.6
E	2.0
F	2.4
G	2.8
H	3.2

The microhardness profiling was taken using a Vickers microhardness indenter (MH-3; Metkon Technology) with a load of 500 g and a dwell time of 15 seconds. The distance between the indentations was maintained at 12 μm.

The tribological property was studied using the ball on disk tribotester (UMT-2; Bruker Corporation) with tungsten carbide ball of diameter 10 mm. A load of 25 N, sliding distance of 2000 m and sliding speed of 0.02 m/s were used during the wear test. The tests were conducted in the dry air without lubrication. The coefficient of friction data were obtained for all the samples. To obtain the wear volume the surface profile of the wear tracks were measured using a stylus surface analyser (Hommel-Etamic W5; Jenoptik, A.G.), with the measuring condition set as follows: effective measured length at 4.8 mm, the cut-off length at 0.8 mm, the measuring range at 400 μm and at a speed of 0.50 mm/s. The wear volume were determined from these surface profiles

3 RESULTS AND DISCUSSION

3.1 Microstructural evaluation and microhardness analysis

The SEM micrograph of the TiC, Ti6Al4V powder and the Ti6Al4V substrate used in this study are shown in Figure 2. The TiC powder particle (see Figure

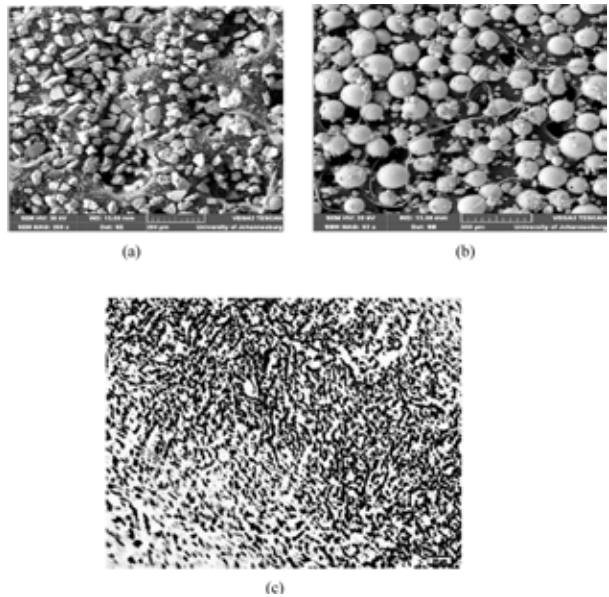

FIGURE 2
SEM micrographs showing (a) the morphology of the TiC powder, (b) the morphology of the Ti6Al4V powder and (c) a micrograph of the surface of the substrate.

2(a)) is characterized by irregular shape morphology while the Ti6Al4V powder particle is spherical in shape (see Figure 2(b)). The microstructure of the surface of the Ti6Al4V substrate (see Figure 2(c)), is characterized by a finely dispersion of alpha grains in the matrix of beta grain structure. The brighter phase showed the alpha grains, while the darker phase indicates the beta grains.

The micrograph of the composite of a sample at laser power of 1.6 kW is shown in Figure 3. The micrograph in Figure 3(a) shows the deposit zone, the interface zone and the heat affected zone. The deposit zone consists of the TiC/Ti6Al4V composite and some un-melted carbides (UMC). The interface zone is where the deposit is bonded to the substrate. Some intermixing of the deposit materials and the substrate material occur in the interface region. This intermixing creates a metallurgical bonding between the deposit and the substrate. The heat affected zone contains only the substrate material that has been affected by the heat of deposition. The heat affected zone is characterized by globular grain structure. The heat transferred from the melt pool causes grain growth in the surrounding grains of the substrate.

The substrate serves as a heat sink for the melt pool directional solidification. The size of the globular grains reduced across the depth of the substrate. The grains that are far away from the interface received less heat from the melt pool. This resulted in the smaller grain growth, and hence the smaller globular grains observed.

Figure 3(b) shows the higher magnification of the interface shown in the Figure 3(a). The interface zone, at higher magnification, shows the dendritic TiC and some resolidified carbides (RSC). The higher magnification of the deposit zone also revealed the dendritic TiC and some RSC as shown in Figure 3(c). The RSC are also referred to as equiaxed TiC grains.

The quantity of the UMC was found to be very high in the sample at a laser power of 0.4 kW and reduces as the laser power was increased. The microhardness profiling result is shown in Figure 4. It was found that the bulk of the UMC observed at a lower laser power of 0.4 kW and 0.8 kW did not lead to an increase in the hardness. The UMC at lower laser powers were not providing the required reinforcing properties, because of the many loose or not well bounded UMC. The loose UMC are detrimental to the wear property of the composite. Because the loose UMC causes scratches which lowers the microhardness when compared to that of the substrate.

It was observed that the microhardness increased as the laser power was increased, until the laser power reached 2.0 kW. As the laser power was further increased beyond 2.0 kW, the microhardness started to decrease. The reason for this behaviour can be attributed to the fact that, as the laser power was increased beyond 2.0 kW, more TiC powder was melted. To improve the surface performance of the substrate, there must be a moderate quantity of UMC. At higher laser power, more carbide powder was melted, which resulted in less UMC in the composite. The low quantity of the UMC provides less rein-

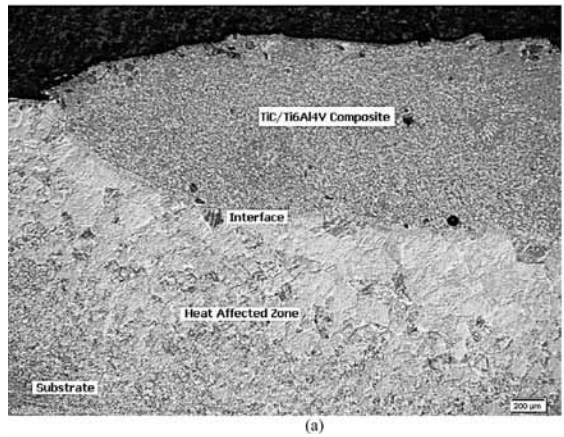

(a)

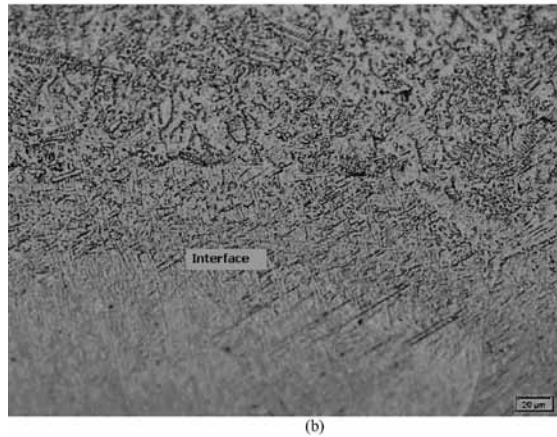

(b)

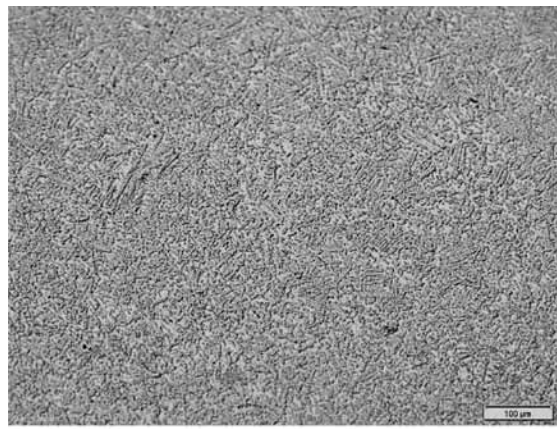

(c)

FIGURE 3
Optical micrographs of the sample deposited at a laser power 1.6 kW (Sample D) showing (a) the deposit layer and the substrate, (b) the interface between the deposit and the substrate and (c) the deposit area at higher magnification.

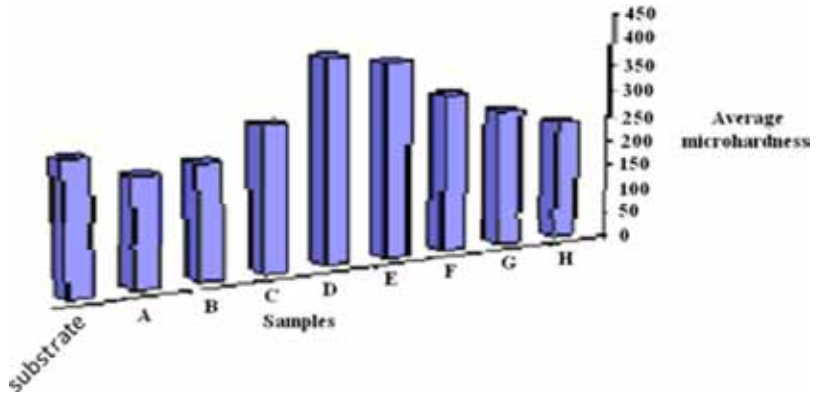

FIGURE 4
Bar chart of the microhardness results of the parent material and the Samples A to H.

forcement for the composite. This shows that there is a limit to which the laser power should be increased in order to retain the required UMC and to improve the microhardness of the composite.

3.2 Wear performance

The dry sliding wear test was performed on all the samples. The worn surfaces were characterized using the SEM, EDS and X-Ray diffraction. Figure 5(a) shows the worn surface of the substrate and Figure 5(b) shows the higher magnification of the morphology of the wear track shown in Figure 5(a). It was observed that there are ploughing grooves on the wear track with some of the loose debris seen. This micrograph shows that the wear mechanism on the substrate material is a combination of abrasion, adhesion and plastic deformation.

At the beginning of the wear test, the tungsten carbide ball comes in contact with the surface of the substrate, resulting in the rubbing of the two surfaces. As the rubbing continues, due to the friction between the two surfaces (no lubrication), and also the property of Ti6Al4V (reacting with the surface in contact) resulted in strong adhesion. This strong adhesion caused rise in temperature that resulted in loose debris. The formation of the debris further aggravated the wear action, by changing the wear mechanism from two-body to three-body wear mechanism. As the sliding continued, these wear debris became work hardened and welded to the two surfaces (the tungsten carbide ball and the wear track of the Ti6Al4V). Causing the characteristic parallel grooves that is typical of abrasive wear mechanism. The wear behaviour exhibited by the substrate material is different from the behaviour observed in the TiC/Ti6Al4V composites.

Figure 6(a) shows the SEM micrograph of the surface of the sample prodcued at a laser power of 2.0 kW before the wear test. Figure 6(b) shows

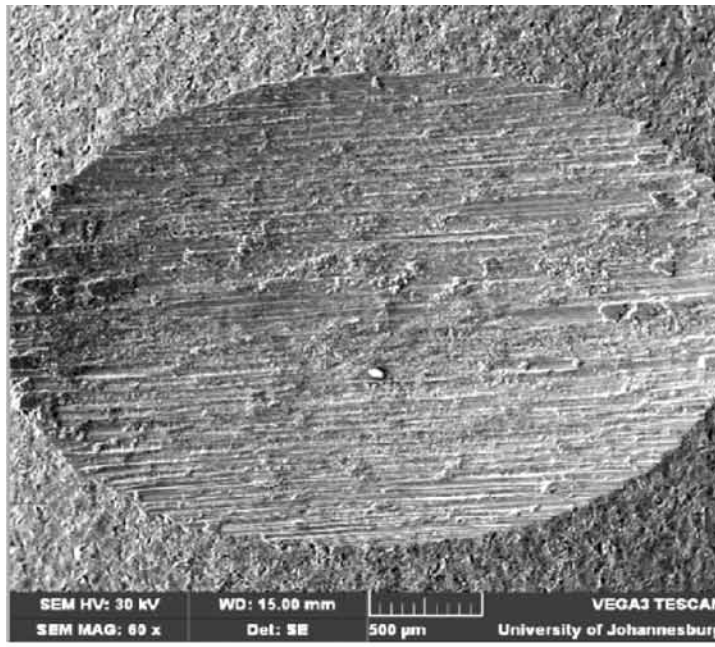

(a)

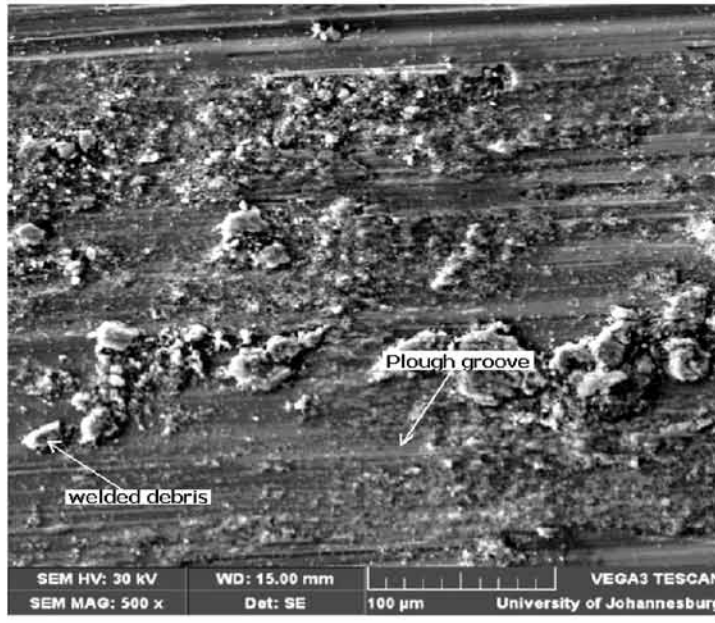

(b)

FIGURE 5
The SEM micrograph of the wear track of the substrate at (a) low magnification (b) higher magnification.

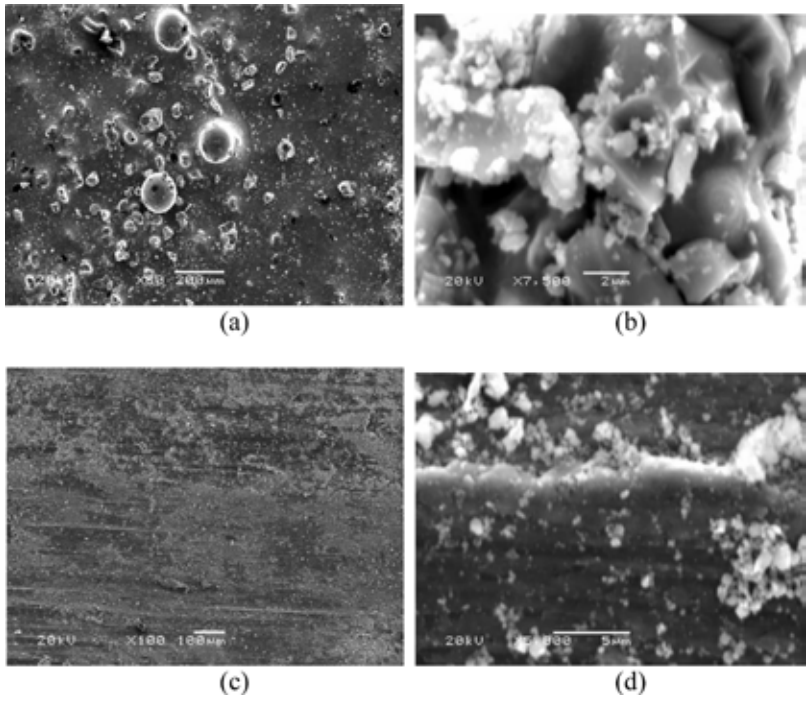

FIGURE 6
SEM micrographs of a sample deposited at a laser power of 2.0 kW (Sample E) showing (a) the surface before wear test, (b) micrograph shown in (a) at higher magnification, (c) the wear track after the wear test and (d) the micrograph shown in (c) at higher magnification.

the higher magnification of the micrograph in Figure 6(a). The wear track of the sample prodcued at the laser power of 2.0 kW is shown in Figure 6(c). The higher magnification of the wear track in Figure 6(c) is shown in Figure 6(d). The SEM micrograph of the sample prodcued at 0.8 kW is shown in Figure 7.

It was found that there is no obvious adhesion of the debris on the wear tracks seen in Figure 6 and Figure 7. This is because, the wear debris from these samples are formed from the hard particle of the UMC of the TiC powder. The three-body wear mechanism that occurred with the TiC/Ti6Al4V composite was such that, the loose debris rubs on the surface containing the embedded UMC. This continuous rubbing resulted in the grinding of this debris and the embedded UMC powder. This rubbing action creates a form of lubrication thereby inhibiting the ploughing action of the debris. It was observed that the wear resistance was not improved at lower laser power. The reason for this is that, there was large quantity of un-melted TiC particles in this samples which were easily removed during the sliding process (see Figure 7). Also, at a very high laser power (above 2.0 kW), the popula-

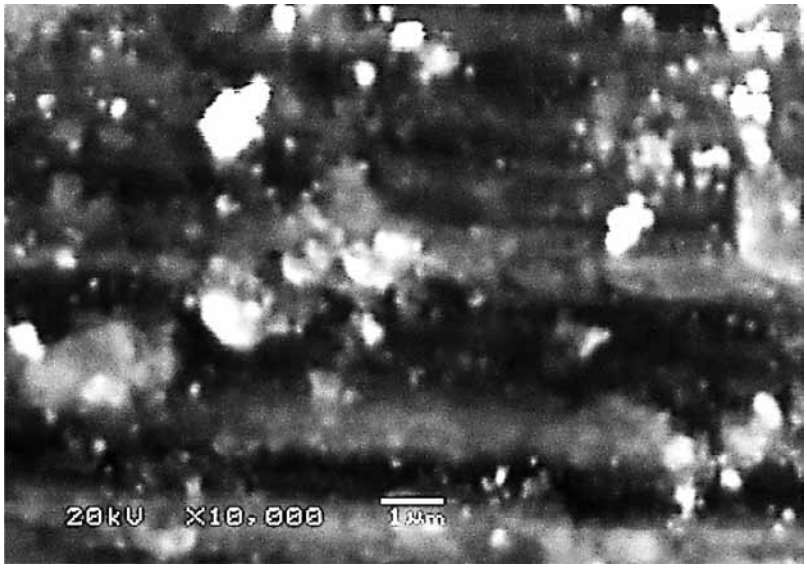

FIGURE 7
SEM micrograph of wear track of a sample treated with a laser power of 0.8 kW (Sample B).

tion of the UMC was reduced. Most of the TiC powders were completely melted at these high laser powers, leaving very few UMC for the reinforcement. Figure 8 shows the SEM micrograph of the sample prodcued at laser power of 2.4 kW. Figure 8(a) shows the micrograph of the surface before the sliding wear test was performed. Figure 8(b) shows the wear track after the sliding wear test. Figure 8c shows the higher magnification of the wear track in Figure 8(b). Figure 8(d) shows the EDS spectrum analysis of the Spot A in Figure 8(c).

The wear resistance was reduced, as shown in Figure 8 because of the lower quantity of the UMC. The quantity of the UMC reduced due to more melting of the TiC powder at higher laser power. The higher laser power caused more TiC powder to be fully melted when compared to the samples at a laser power of 1.6 and 2.0 kW. At a laser power of 2.0 kW, the UMC was well bonded in the matrix of the Ti6Al4V grains and serves as a powder lubricant during the sliding wear process. The protruding UMC were cut off from the surface of the composite forming a three-body wear mechanism. Instead of the loose debris further cutting deep into the surface, they were ground into fine powder. The hard particles of the embedded UMC continue to rub the debris thereby reducing the size of the debris into a finer particles. These fine particles of the debris separated the two surfaces in contact (the tungsten carbide ball and the composite) forming what looks like a powder lubricant; hence the fine powder improved the wear resistance. Most of the TiC powders were dissolved into the Ti6Al4V matrix as a result of been melted by the

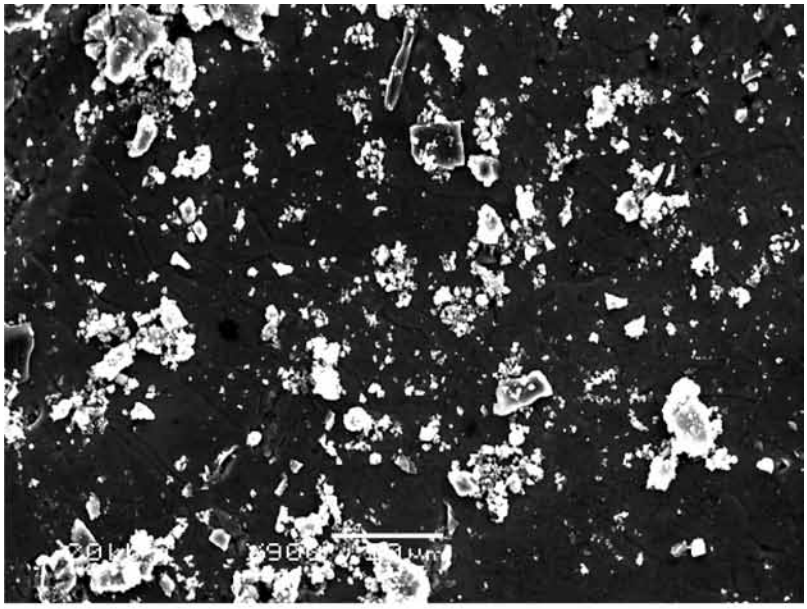

(a)

(b)

FIGURE 8
SEM micrographs of a sample deposited at a laser power of 2.4 kW (Sample F) showing (a) the surface before the wear test, (b) the wear track after the wear test,

Continued

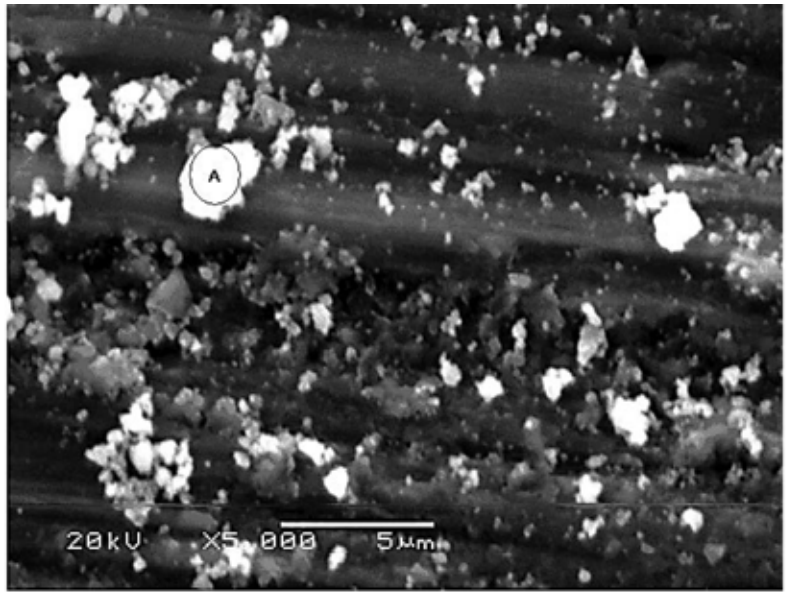

(c)

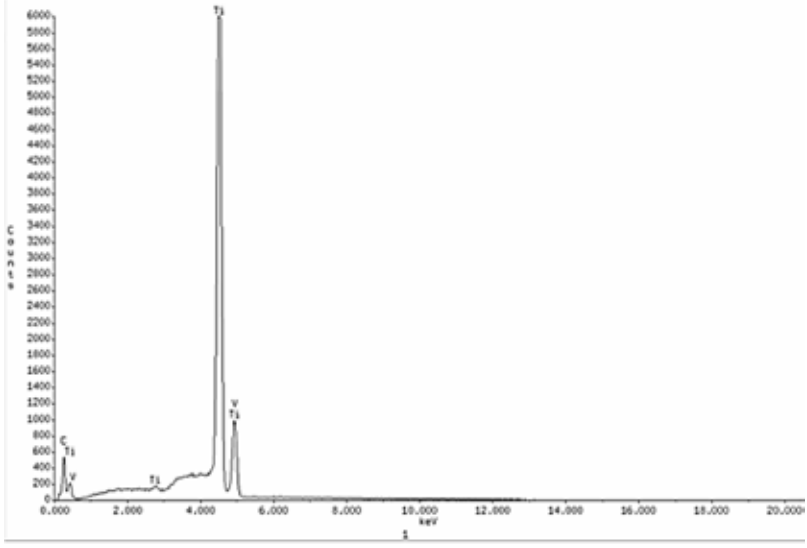

(d)

FIGURE 8
(c) the micrograph shown in (b) at higher magnification and (d) the EDS analysis of the Point A in the micrograph shown in (c).

higher laser power of 2.4 kW (see Figure 8). During the sliding wear process, the loose debris from the few UMC was not only rubbing the embedded UMC alone, it was also rubbing the matrix containing the dissolved TIC. The matrix containing dissolved TiC is soft, and instead of the loose debris to reduce in size they continued to cut deeper groves. That was why the wear resistance was not improved at higher laser powers when compared to the samples produced at 1.6 and 2.0 kW laser powers. The EDS spectrum at Spot A, in Figure 8(c), as shown in Figure 8(d) confirms that the spot is a mixture of TiC and Ti6Al4V.

The plot of the coefficient of sliding friction of all the samples under investigation against the sliding distance is presented in Figure 9(a). To be able to see and compare the coefficient of friction, fewer samples are shown in Figure 9(b). Also the bar chats of the wear volume of all the samples and the substrates are shown in Figure 9(c).

The plot of the coefficient of friction and the bar chat of the wear volume show that the best wear resistance occurred in the sample E, at a laser power of 2.0 kW. The coefficient of friction and the wear volume show similar trend because of the wear condition employed in this study. The optimum power to produce the composite with the most improved wear resistance property is 2.0 kW, based on the processing parameters employed in this study. Below and above this laser power, the wear resistance performances reduced. This shows that at 2.0 kW, a reasonable amount of the UMC was retained in the matrix of the Ti6Al4V substrate. The retained UMC was capable of improving the sliding wear resistance property of the composite. To further confirm this result, the XRD analysis was performed on the samples at laser powers of 1.6 and 2.0 kW. The XRD result is shown in Figure 10. The XRD results were correlated to the wear resistance behaviour analysis. It was observed that the samples produced at 2.0 kw which has a higher density of the 4 mc compared to the samples produced at 1.6 kw has the best wear resistance.

4 CONCLUSIONS

The following conclusions can be drawn from this work:

(i) TiC/Ti6Al4V composite of 50 wt.% ratio has been successfully deposited. The effect of varying the laser power on the resulting properties of the composite has been investigated.
(ii) The microhardness and the wear resistance were found to be dependent on the laser power. The microhardness and the wear resistance increased

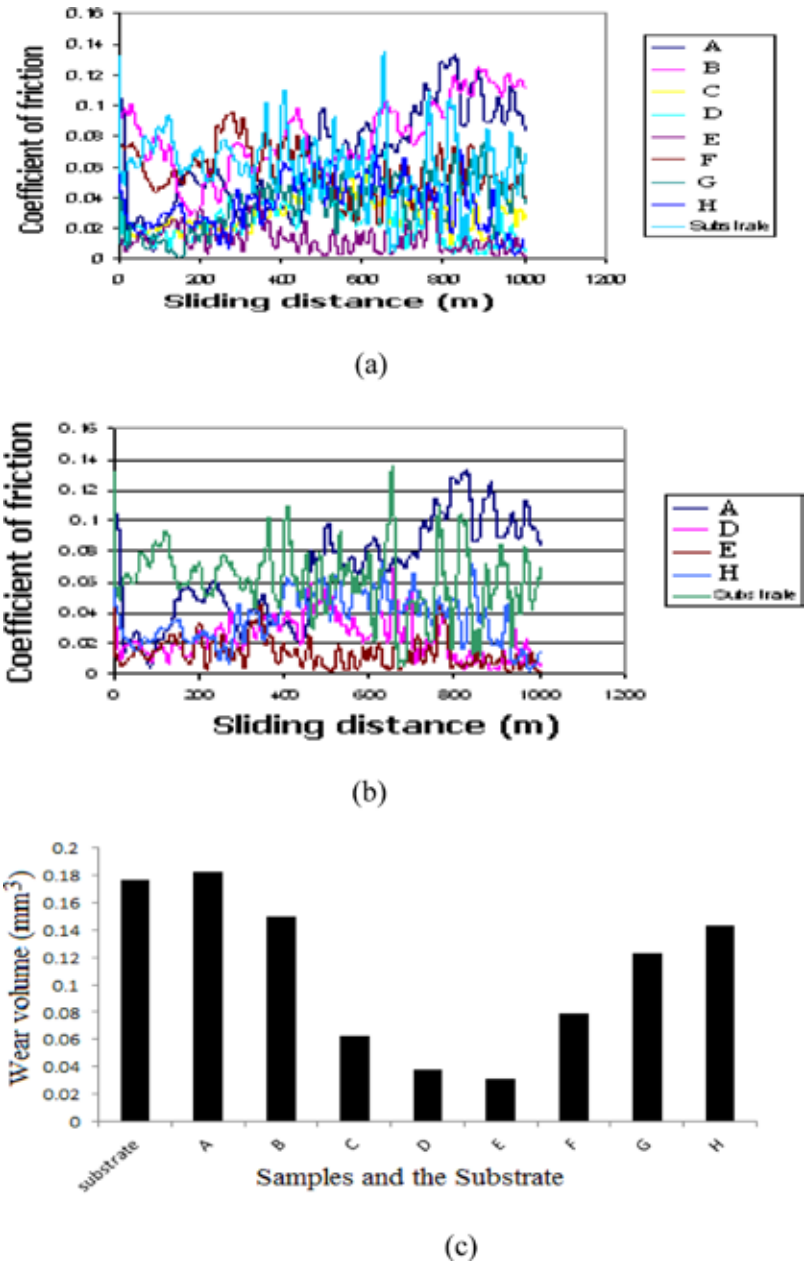

FIGURE 9
Plots of the coefficient of friction against the sliding distance of samples (a) A to H; (b) A, D, E and H and (c) the bar chat of the wear volume.

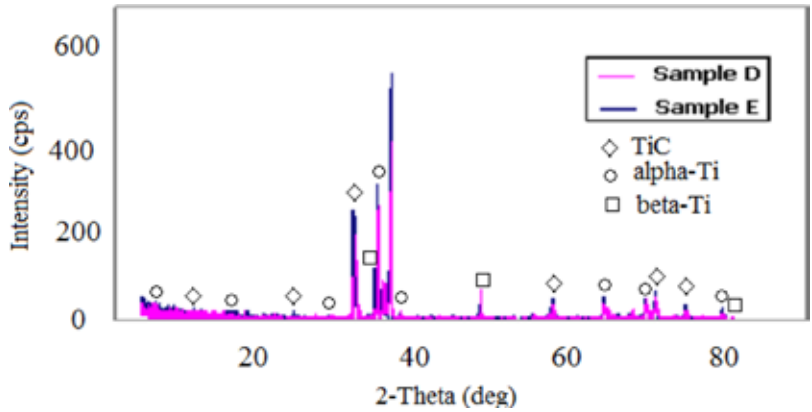

FIGURE 10
XRD spectra of a samples treated with a laser power of 1.6 kW (Sample D) and 2.0 kW (Sample E).

initially as the laser power was increased from 0.4 to 2.0 kW and then experienced a decrease as the laser power was further increased.

(iii) Further increase in the power beyond 2 kW reduced the quantity of the un-melted carbide (UMC) and this reduced the wear resistance performance of the TiC/Ti6Al4V composites.

(iv) It can be concluded that the optimal laser power requirement for better wear resistance performance is 2 kW for the set of processing parameters considered in this study.

ACKNOWLEDGMENTS

This work is supported by the Rental Pool Programme of National Laser Centre**,** Council of Scientific and Industrial Research (CSIR)**,** Pretoria, South Africa and The Schlumberger Foundation Faculty for the Future (FFTF).

REFERENCES

[1] Scott J., Gupta N., Wember C., Newsom S., Wohlers T. and Caffrey T. (2012). *Additive manufacturing: status and opportunities, Science and Technology Policy Institute*, Retrieved 11th July 2012, from https://www.ida.org/stpi/occasionalpapers/papers/AM3D_33012_Final.pdf

[2] Wu X., Liang J., Mei J., Mitchell C., Goodwin P.S. and Voice W. Microstructures of laser-deposited Ti–6Al–4V. *Materials & Design* **25**(2) (2004), 137–144.

[3] Fink C.W. An overview of additive manufacturing Part II. *AMMTIAC Quarterly* **4**(3) (2009), 7–10.

[4] Brandl E., Michailov V., Viehweger B. and Leyens C. Deposition of Ti-6Al-4V using laser and wire, Part I: Microstructural properties of single beads. *Surface & Coatings Technology* **206**(6) (2011), 1120–1129.

[5] Lu Y., Tang H.B., Fang Y.L., Liu D. and Wang H.M. Microstructure evolution of sub-critical annealed laser deposited Ti–6Al–4V alloy. *Materials & Design* **37** (2012), 56–63.

[6] Ezugwu E.O. and Wang Z.M. Titanium alloys and their machinability: A review. *Journal of Materials Processing Technology* **68**(3) (1997), 262–274.

[7] Dalili N., Edrisy A., Farokhzadeh K., Li J., Lo J. and Riahi A.R. Improving the wear resistance of Ti–6Al–4V/TiC composites through thermal oxidation (TO). *Wear* **269**(7) (2010), 590–601.

[8] Wang F., Mei J., Jiang H. and Wu X. Laser fabrication of Ti6Al4V/TiC composites using simultaneous powder and wire feed. *Materials Science and Engineering A Structural Materials: Properties, Microstructure and Processing* **445-446** (2007), 461–466.

[9] Wang F., Mei J. and Wu X. Compositionally graded Ti6Al4V + TiC made by direct laser fabrication using powder and wire. *Materials & Design* **28**(7) (2007), 2040–2046.

[10] Tian Y.S., Chen C.Z., Li S.T. and Huo Q.H. Research progress on laser surface modification of titanium alloys. *Applied Surface Science* **242**(1-2) (2005), 177–184.

[11] Zhang K., Zou J., Li J., Yu Z. and Wang H. Surface modification of TC4 Ti alloy by laser cladding with TiC+Ti powders. *Transactions of Nonferrous Metals Society of China* **20**(11) (2010), 2192–2197.